

*LIGO Laboratory / LIGO Scientific Collaboration*

LIGO-T080064-v1-D

*Advanced LIGO*

3/10/08

---

Controlling Light Scatter in Advanced LIGO

---

Dan Riley and Michael Smith

Distribution of this document:  
LIGO Science Collaboration

This is an internal working note  
of the LIGO Project.

**California Institute of Technology**  
**LIGO Project – MS 18-34**  
**1200 E. California Blvd.**  
**Pasadena, CA 91125**  
Phone (626) 395-2129  
Fax (626) 304-9834  
E-mail: [info@ligo.caltech.edu](mailto:info@ligo.caltech.edu)

**Massachusetts Institute of Technology**  
**LIGO Project – NW17-161**  
**175 Albany St**  
**Cambridge, MA 02139**  
Phone (617) 253-4824  
Fax (617) 253-7014  
E-mail: [info@ligo.mit.edu](mailto:info@ligo.mit.edu)

**LIGO Hanford Observatory**  
**P.O. Box 1970**  
**Mail Stop S9-02**  
**Richland WA 99352**  
Phone 509-372-8106  
Fax 509-372-8137

**LIGO Livingston Observatory**  
**P.O. Box 940**  
**Livingston, LA 70754**  
Phone 225-686-3100  
Fax 225-686-7189

<http://www.ligo.caltech.edu/>

**Table of Contents**

**1 Introduction** ..... 4

**2 SURF Report, Dan Riley, 10/31/07** ..... 5

**Table of Figures**

*Figure 1 - Scattered light inside Advanced LIGO* ..... 5

*Figure 2 - BRDF definition diagram<sup>1</sup>* ..... 6

*Figure 3 - Scatterometer layout* ..... 6

*Figure 4 - Lambertian Scatterer BRDF* ..... 7

*Figure 5 - BRDF comparison of several samples* ..... 8

*Figure 6 - Ray trace of sample scatter and beam dump scatter* ..... 8

*Figure 7 – Dust particles on sample surface as seen by video camera* ..... 8

**Abstract**

A significant issue in the Advance LIGO interferometer is the amount of scattered light. One purpose of the Auxiliary Optics Support (AOS) subsystem is to control and minimize the scattered light in the interferometer through the use of optical components such as baffles and beam dumps. Although these components significantly reduce scattered light, they also have inherent levels of scatter due to material composition and geometry. The light scatter from the AOS components can introduce noise into the LIGO detectors because they are not seismically isolated. In order to quantify the amount of scattered light and to qualify materials for use in AOS, we have constructed a highly sensitive scatterometer capable of measuring the Bidirectional Reflectance Distribution Function (BRDF) and the reflectivity of a material. We were able to verify the design concept of the scatterometer using a calibrated lambertian scattering surface. The materials of primary interest were black welder's glass, a super polished Brewster window, Laser Black 3188, and several types of oxidized stainless steel. We were able to achieve the sensitivity necessary to measure the BRDF and reflectivity of all the materials of interest. The material with the lowest BRDF was black glass with a  $BRDF < 10^{-6}$

## **1 Introduction**

This note summarizes the measured BRDF and reflectivity properties of various materials for use in Advanced LIGO. This report is a submission of the SURF report by Dan Riley on 10/31/07.

## 2 SURF Report, Dan Riley, 10/31/07

## Controlling Light Scatter in Advanced LIGO

AUTHOR: D. RILEY

MENTOR: M. SMITH

A significant issue in the Advance LIGO interferometer is the amount of scattered light. One purpose of the Auxiliary Optics Support (AOS) subsystem is to control and minimize the scattered light in the interferometer through the use of optical components such as baffles and beam dumps. Although these components significantly reduce scattered light, they also have inherent levels of scatter due to material composition and geometry. The light scatter from the AOS components can introduce noise into the LIGO detectors because they are not seismically isolated. In order to quantify the amount of scattered light and to qualify materials for use in AOS, we have constructed a highly sensitive scatterometer capable of measuring the Bidirectional Reflectance Distribution Function (BRDF) and the reflectivity of a material. We were able to verify the design concept of the scatterometer using a calibrated lambertian scattering surface. The materials of primary interest were black welder's glass, a super polished Brewster window, Laser Black 3188, and several types of oxidized stainless steel. We were able to achieve the sensitivity necessary to measure the BRDF and reflectivity of all the materials of interest. The material with the lowest BRDF was black glass with a BRDF on the order of  $10^{-8}$ .

Although the AOS subsystem is capable of reducing the scattered light in Advanced LIGO by many orders of magnitude, the extreme sensitivity of the interferometer requires that the light that is again scattered off the AOS components be quantified and minimized. The light scattered by an AOS component is simplistically demonstrated in Figure 1. The strength of this noise signal is estimated by the following equation:

$$\text{Noise} = E_{\text{scat}} \frac{4\pi X_{\text{scat}}}{\lambda} \quad (1)$$

$E_{\text{scat}}$  is the electric field of the light scattered from an AOS component.  $X_{\text{arm}}$  is the amount that the component moves due to factors such as thermal activity and seismic vibrations, and  $\lambda$  is the wavelength of the LIGO laser. The gravity wave signal strength can also be estimated by eq. 1, with  $E_{\text{scat}}$  replaced by the electric field in the interferometer arm, and  $X_{\text{scat}}$  replaced by the amount the length of the arm changes due to the gravity wave. The noise-to-signal ratio gives us

$$\frac{\text{Noise}}{\text{Signal}} = \frac{E_{\text{scat}} X_{\text{scat}}}{E_{\text{arm}} X_{\text{arm}}} = \sqrt{\frac{P_{\text{scat}} X_{\text{scat}}}{P_{\text{arm}} X_{\text{arm}}}} \quad (2)$$

Eq. 2 tells us that the noise-to-signal ratio is equal to ratio of the movement of the scattering surface to the interferometer arm length change times the square root of the ratio of the power of the scattered light to the power of the light in the arm. The only unknown quantity in eq. 2 is  $P_{\text{scat}}$ . In order to determine  $P_{\text{scat}}$  we need to know the Bidirectional Reflectance Distribution Function (BRDF) of a material. Eq. 3 describes the relationship between the BRDF and  $P_{\text{scat}}$ .

$$P_{\text{scat}} = P_{\text{inc}} * \Delta\Omega * \text{BRDF} \quad (3)$$

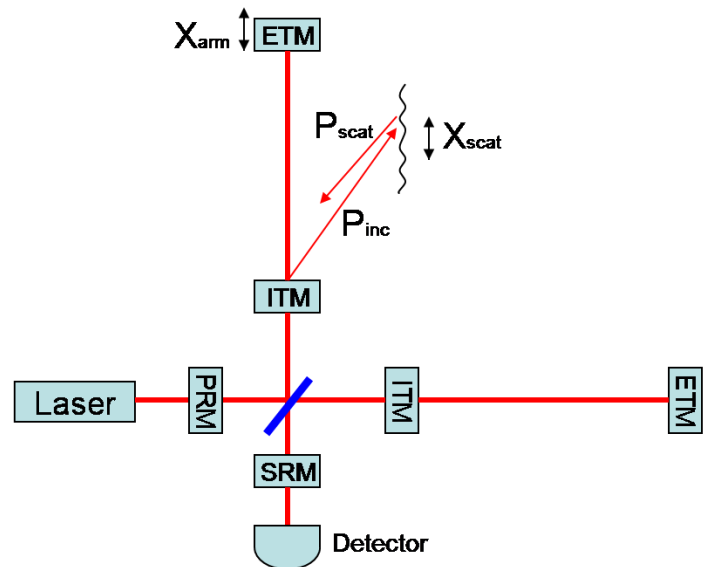


Figure 1 - Scattered light inside Advanced LIGO

$\Delta\Omega$  is the solid angle of the gravity wave signal detector and  $P_{\text{inc}}$  is the power of the light signal scattered by the interferometer that the AOS is attempting to eliminate.

The BRDF is the ratio of the differential radiance to the differential irradiance of a sample. In other words it is the ratio of the light power incident on a surface to the light power scattered from that surface through a solid angle. We use the following equation to determine the BRDF:

$$\frac{\text{Irradiance}}{\text{Radiance}} \approx \frac{\left(\frac{P_i}{A}\right)}{\left(\frac{P_s}{\Delta\Omega \cos\theta_s}\right)} = \left(\frac{P_s}{P_i \Delta\Omega}\right) \frac{1}{\cos\theta_s} = \frac{\text{BRDF}}{\cos\theta_s} \quad (4)$$

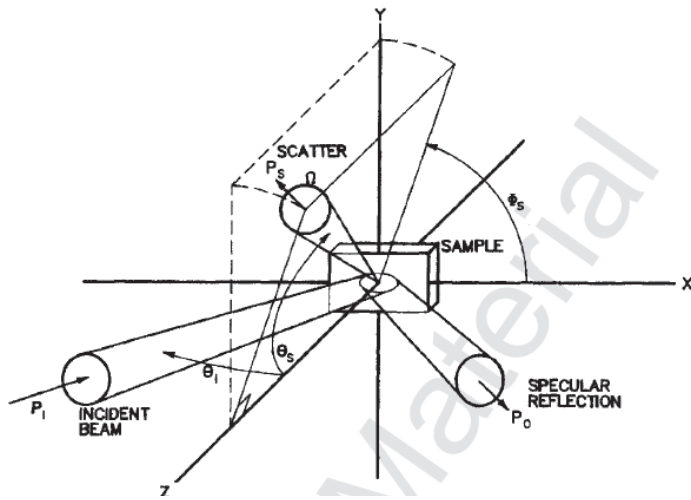


Figure 2 - BRDF definition diagram<sup>1</sup>

The cosine term from the radiance definition is not included in the BRDF, because we chose to measure the “cosine corrected” BRDF. A visual example of what the BRDF is can be found in Figure 2.

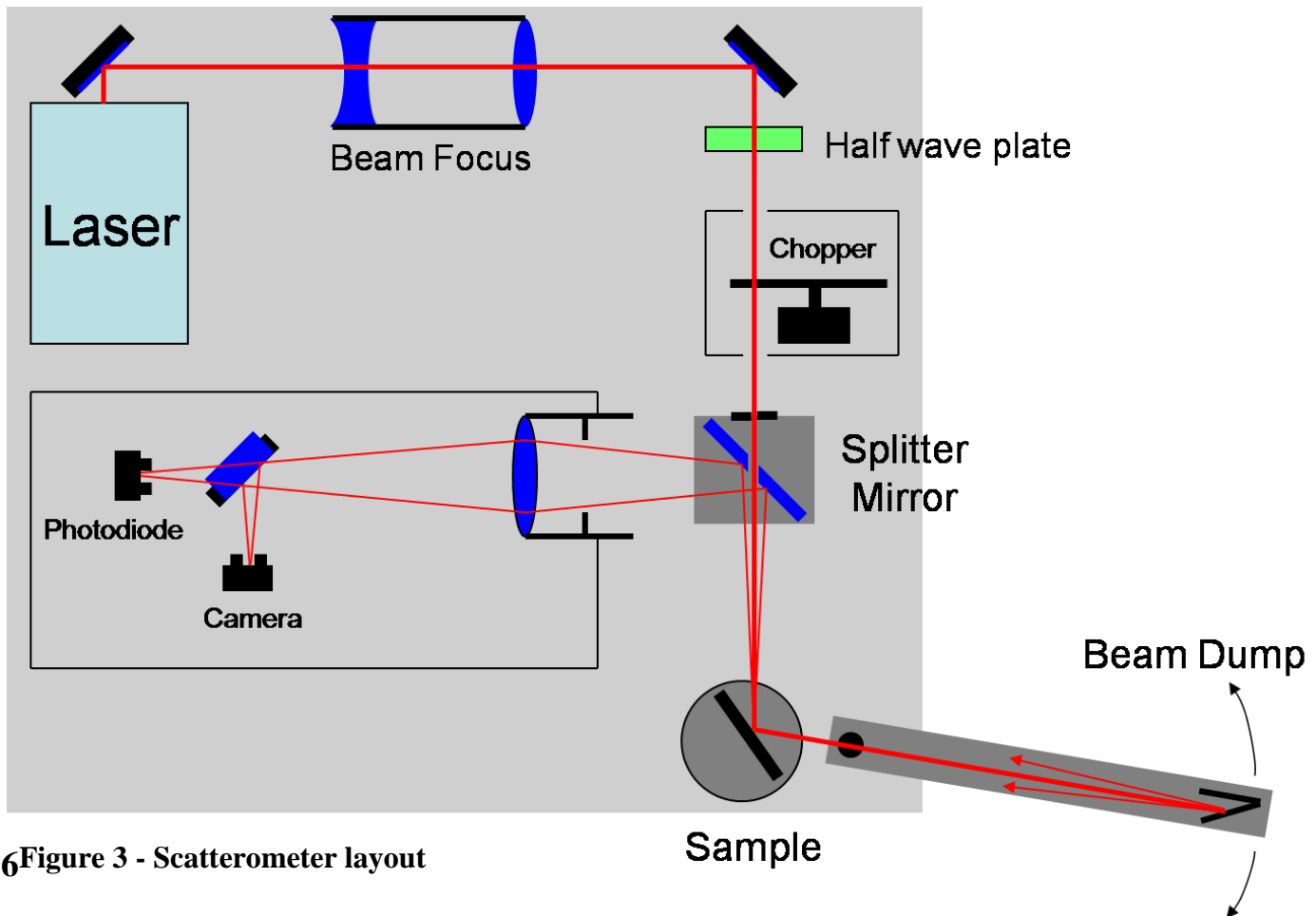
Although the BRDF is a function of the incident angle of the beam and the scattering angle, we are only interested in backscattered light, because this is the light that has potential to enter one of the main detectors. The BRDF measurement is then a function of only the incidence angle, and the scattering angle is approximately zero relative to the incident beam.

According to scatter theory the BRDF is directly proportional to the reflectivity of the scattering sample. Polarization and incidence angle are both closely related to the reflectivity, especially at Brewster’s angle where an S-polarized electromagnetic wave will strongly couple into and be absorbed by the surface of the scattering material. As a result all measurements were made with both S-polarization and P-polarization.

SCATTEROMETER

A diagram of the scatterometer we built to measure the BRDF can be found in Figure 3. It begins with a high power laser source to create a laser beam that is reflected off two steering mirrors. The beam passes through the “Beam Focus” which is a pair of telescopic lenses used to create a beam waist at the sample location. The beam then passes through a half-wave plate to rotate the polarization and a chopper wheel. The chopper wheel modulates the beam signal to allow any noise in the signal to be rejected. The beam then passes through a small metal hole and then through a second hole in the back of a mirror and hits the sample. The purpose of the metal hole is to reduce to radius of the beam to smaller than the hole in the mirror to ensure that no light is scattered off the inside of the hole in the mirror. This is crucial because the surface of the mirror is in direct line of sight of the photodiode.

A beam dump on an arm that can be rotated around the sample is then positioned to catch the specular reflection. The backscattered light is reflected by the “Splitter Mirror” through an adjustable aperture, which is used to set the solid angle for the BRDF calculation. The backscattered light is then focused onto a photodiode to form an image of the scattering spot from the



6Figure 3 - Scatterometer layout

sample. It also passes through a 50/50 beam splitter onto a camera. The camera allows us to view the surface of the sample to ensure there are no dust particles causing scatter. The signal from the photodiode is sent to a lock-in amplifier which uses the modulation frequency set by the chopper wheel to reject any noise in the signal.

In order to prove the concept of the scatterometer, we measured the BRDF of a calibrated scattering source called a Lambertian scatterer. This is a perfectly diffuse scattering surface and the BRDF is known to be

$$BRDF = \frac{\cos\theta}{\pi} \quad (5)$$

Figure 4 is a comparison of the theoretical BRDF and our experimental measurement. Our goal was to be able to measure the BRDF to within a factor of 2 because we expected to be measuring it across many orders of magnitude. This graph indicates that the scatterometer is working as expected and accurately.

The reflectivity measurement was straightforward. In order to measure the reflectivity we simply measured the power at the sample and then the power of the specular reflection using a calibrated power meter.

## BRDF AND REFLECTIVITY MEASUREMENTS

BRDF and reflectivity measurements were made for a variety of materials including black glass, a super polished Brewster window, laser black 3188, four different types of oxidized stainless steel, and a polished piece of stainless steel. Figure 5 is a comparison of the BRDF of several of these materials on a logarithmic plot. All of the BRDF plots can be found in Appendix A and the reflectivity plots for black glass and the Brewster window be found in Appendix B.

In Figure 5, notice the extremely low value for the BRDF of black glass. This is an unpolished piece of welder's glass. We did not expect this material to have a lower level of backscatter than the super polished window. It's BRDF on the order of  $10^{-8}$  is extremely low. There is also not a significant

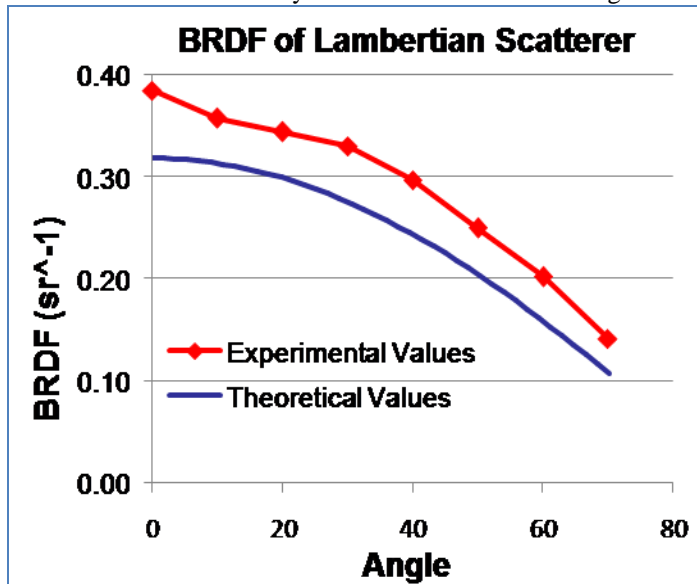


Figure 4 - Lambertian Scatterer BRDF

change in the backscatter of the super polished window or the black glass as the angle approaches Brewster's angle ( $56^\circ$ ).

According to standard scattering theory the BRDF is directly proportional to the reflectivity of the material.<sup>1</sup> The reflectivity plots for the black glass and the super polished window both show significant decreases in the reflectivity as the incidence angle approaches Brewster's angle, therefore we would expect the BRDF to also follow this trend. The behavior of the BRDF is not understood at this point.

Future work for the scatterometer will involve transporting it to Lauritsen. It was built on a bread board with mobility in mind. Caltech will also be obtaining a commercial scatterometer soon, and it will be interesting to compare the results from the two scatterometers. The scatterometer will also be used in the future to measure other materials to be used in LIGO and other applications.

## METHODS

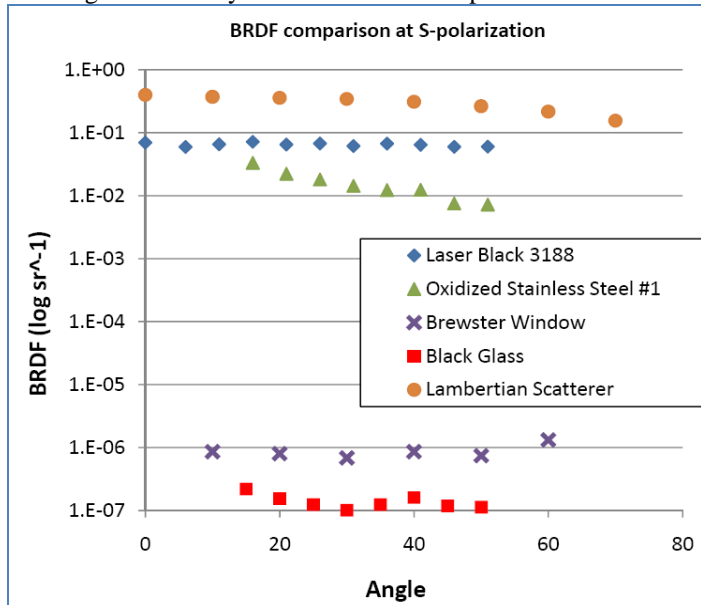
### CUSTOM CONSTRUCTION

Much of the scatterometer was built with parts either designed by us in SolidWorks or AutoCAD and built by the machine shop or built by us. The "splitter mirror" was an especially complicated task. We designed a mount to hold the mirror and the metal aperture behind it. This was attached to a stage that allowed us to rotate the mirror or tilt it in two directions. We also designed a fixture to allow us to drill the hole the mirror needed to allow the beam to pass through. When we received the mirror we applied a coating to it to protect it during the drilling process. We then proceeded to use a diamond drill to carefully drill through the substrate and reflective coating of the mirror at precisely a  $45^\circ$  angle.

Parts were also fabricated to mount the scattering sample and attach it to a rotational stage, as well as rigid mounts for the telescopic lenses and the aperture in front of the focusing lens that determines the solid angle. SolidWorks images of both of these parts can be found in Appendix C.

### LOW SIGNAL DETECTION

One of the greatest challenges in building the scatterometer was reaching a sensitivity on the order of 10 picowatts to measure



The scattered light from the back of the chopper wheel when it blocks the laser is modulated at the exact frequency of the signal we were attempting to measure, but it is 180° out of phase. It was very large relative to backscatter signal, so significant steps had to be taken to minimize the amount of this light reaching the photodiode. In our initial design of the scatterometer we were using a beam splitter in place of a mirror with a hole. Due to how a beam splitter works differently from the mirror we had to place the chopper wheel after the splitter in the path of the beam. The backscatter from the chopper wheel was then reflected directly into the photodiode and wasn't rejected. This made it impossible to make an accurate and precise BRDF measurement.

By using a mirror with a hole, we were able to place the chopper wheel behind the mirror which acted as a "splitter." We then took steps to completely isolate any chopper wheel scatter from the photodiode. The imaging system was also extremely helpful in guaranteeing none of the chopper scatter was hitting the photodiode.

IMAGING

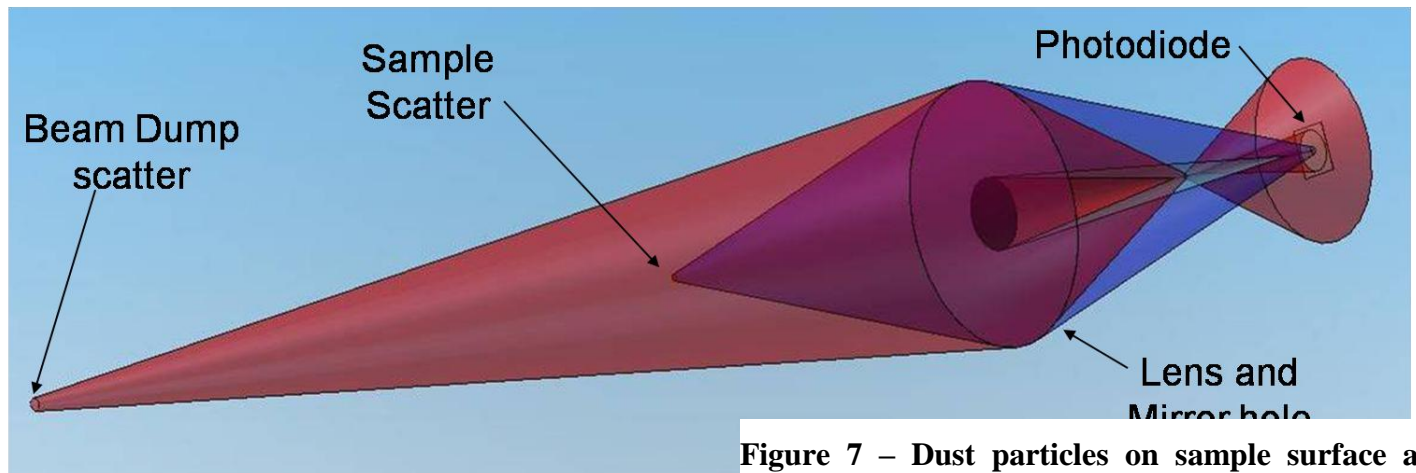


Figure 6 - Ray trace of sample scatter and beam dump scatter

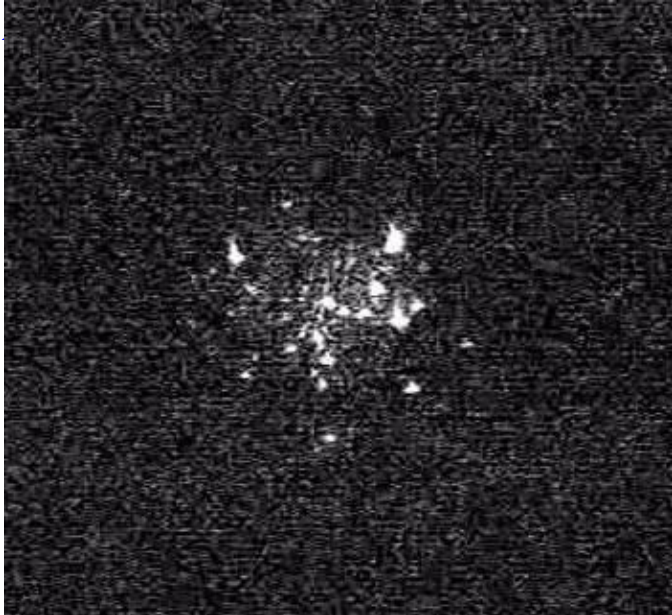
Figure 7 – Dust particles on sample surface as seen by video camera

Figure 5 - BRDF comparison of several samples

extremely low BRDF values. The key to this is the lock-in amplifier. By using it in conjunction with the chopper one can reject huge levels of noise. An unexpected problem we faced early on however was scatter from the chopper wheel itself.

A lens was used to focus an image of the scattering spot onto the photodiode. This was extremely helpful to minimize any noise from the chopper or backscatter from the beam dump receiving the specular reflection. This is demonstrated in Figure 6 which is a model of the rays scattered from the sample and from the beam dump made in SolidWorks.





The blue rays in Figure 6 are backscatter from the sample that we wanted to measure. The red rays are back scatter from the beam dump that would cause noise. At the lens there is an obscuration that represents the hole in the mirror. This hole acts as an obscuration because any rays that reach it will not be reflected to the photodiode. They will simply pass through. The lens forms a one-to-one image of the sample scatter while the image from the beam dump scatter is formed in front of the photodiode. As the rays from the beam dump continue propagating, they form a cone that is absent of any of the beam dump scatter. A very small fraction of beam dump rays end up hitting the photodiode. The area of the cone hitting the photodiode was larger than the area of the sample spot size. We took advantage of this by placing an aperture immediately in front of the photodiode that was large enough to allow all the rays from the sample scatter to hit the photodiode but block all the rays from the beam dump scatter. In addition to this, the beam dump scatter rays have traveled much further than the sample scatter rays, and their intensity reduces by  $1/r^2$ .

### GAUSSIAN BEAM CONTROL

An assumption made in the BRDF calculation is that all rays in the beam hitting the sample are parallel. It is also advantageous for imaging purposes that the beam have a very small radius. Both of these conditions can be satisfied by understanding the propagation of a Gaussian beam and manipulate it using lenses. The ABCD matrix approach was used to create a program in Matlab that would allow us to input various parameters about the optics of the scatterometer and calculate various properties of the beam. Appendix D contains the code used for this program. This program was used to determine what lenses would be used in the “Beam Focus” in figure 3 and how far apart they would be set which is referred to as the “focus length.” The Matlab program generates information such as the beam waist location and beam waist radius as a function of the focus length and the beam radius profile once it exits the Beam Focus. Examples of this information can be found in Appendix E.

### VIDEO CAMERA

The camera used to view the sample scattering spot was extremely important for ensuring a correct measure of the BRDF. Dust on the surface of a material with a very low BRDF

such as black glass can drastically increase the amount of scatter the photodiode detects. Figure 7 shows what the surface of the black glass looks like when there are dust particles causing scatter. These can increase the signal several orders of magnitude. The surface appears perfectly black when there are no dust particles.

### CALIBRATION

The output of the photodiode used to detect the power of the scattered light is an uncalibrated voltage signal. In order to calibrate the photodiode we used a known laser power and neutral density filters. A high scattering surface was placed at the sample location to create a large enough signal at the photodiode for a calibrated meter to measure. This signal is far too strong for the photodiode and easily saturates it, therefore known neutral density filters were placed in front of the photodiode. With a known signal strength and known neutral density filters, we could calculate the power of the signal hitting the photodiode and calibrate the voltage output.

We can measure how much signal is being generated only by the scatterometer and not the sample. This is referred to as the “instrument signature.” This is done by removing the sample from the system and allowing the laser to directly hit the beam dump. We measured an instrument signal of approximately 20 picowatts. This was smaller than the smallest signal we measured, and could therefore be subtracted out as a systematic error.

### REFERENCES

1. Handbook of Optics, Vol. 2. McGraw-Hill Professional, 1994. 26.1-26.8.

### ACKNOWLEDGEMENTS

I like to thank my mentor Mike Smith for providing so much guidance and help and for making sure I had a great research experience at Caltech. I would like to thank LIGO, SURF, and the NSF for creating such a great summer program at Caltech for students like me and for funding my research.

## APPENDIX A

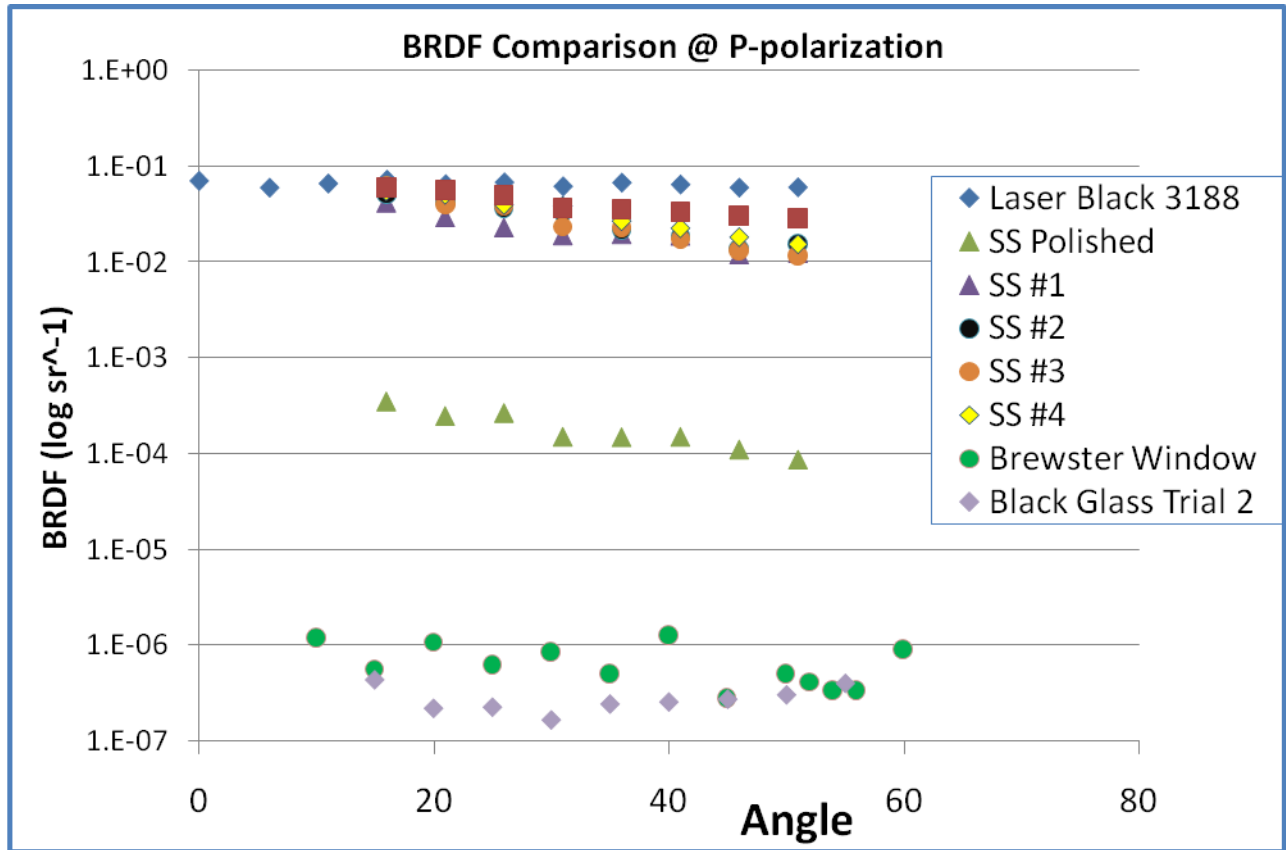


Figure A 1 - BRDF of samples measured with P-polarization

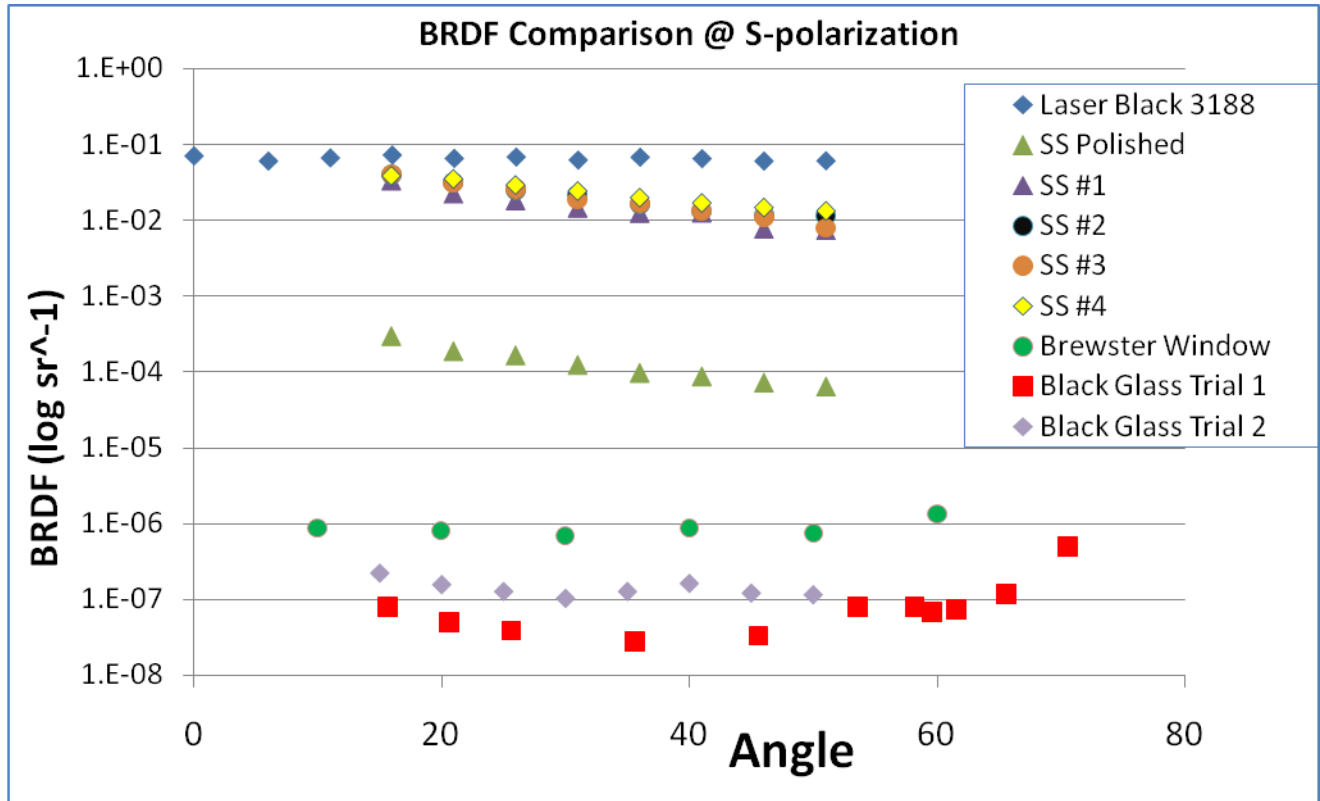


Figure A 2 - BRDF of samples measured with S-polarization

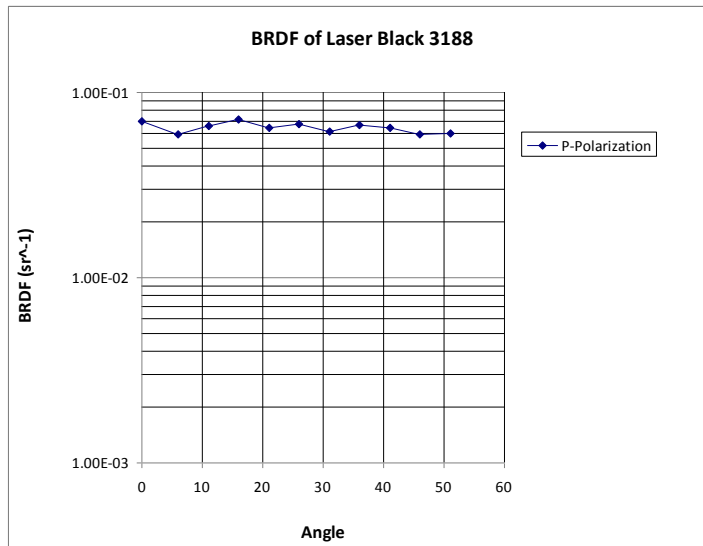


Figure 8 – BRDF of laser black 3188

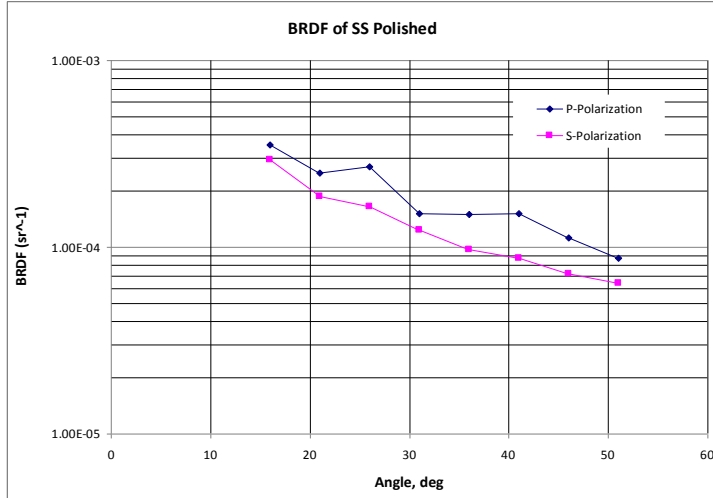


Figure 9 – BRDF of polished stainless steel

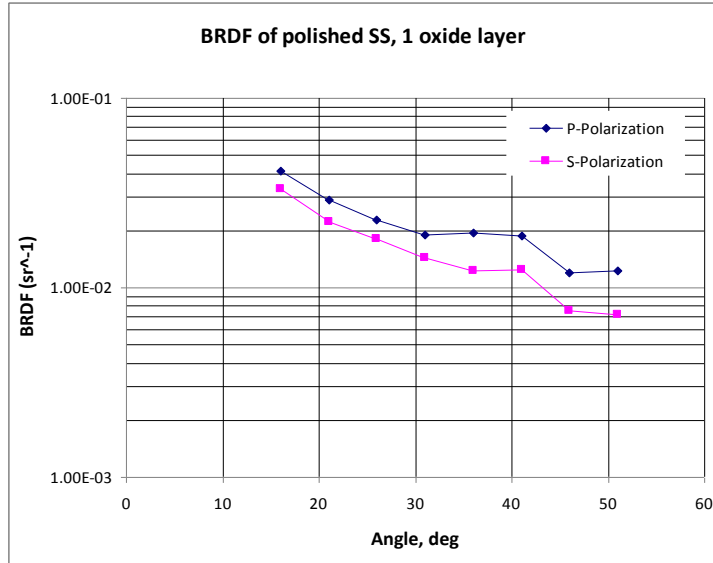


Figure 10 – BRDF of polished stainless steel with 1 oxide layer

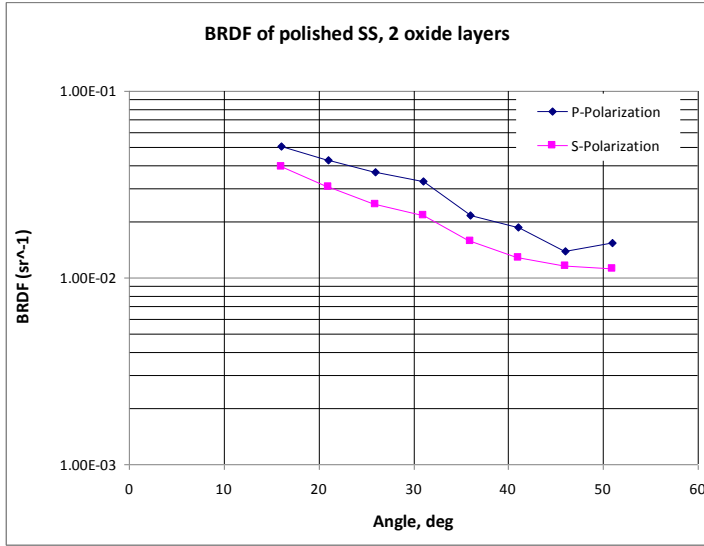


Figure 11 – BRDF of polished stainless steel with 2 oxide layers

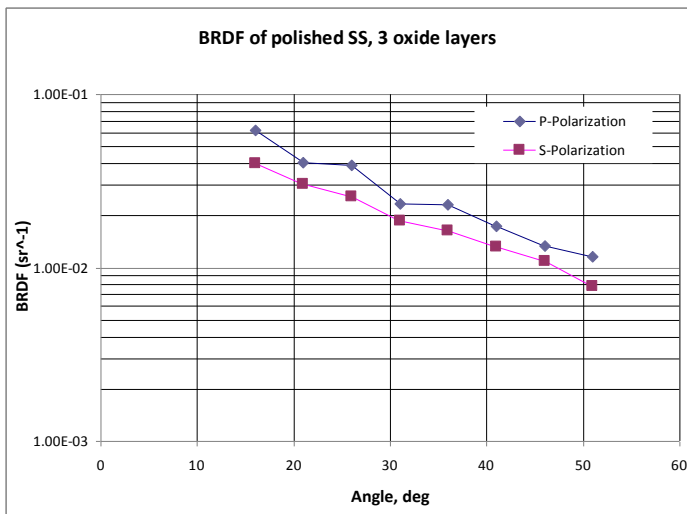


Figure 12 – BRDF of polished stainless steel with 3 oxide layers

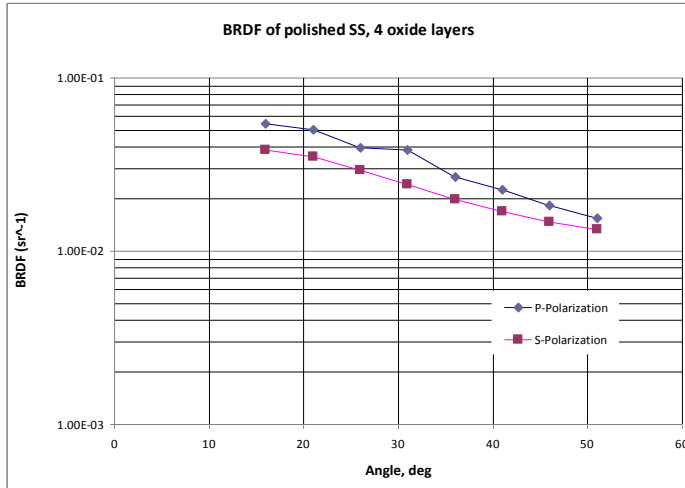


Figure 13 – BRDF of polished stainless steel with 4 oxide layers

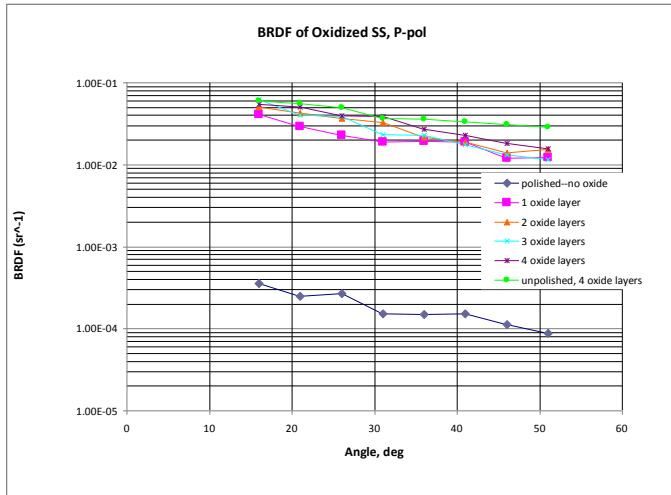


Figure 14 – BRDF of oxidize stainless steel samples at P-polarization

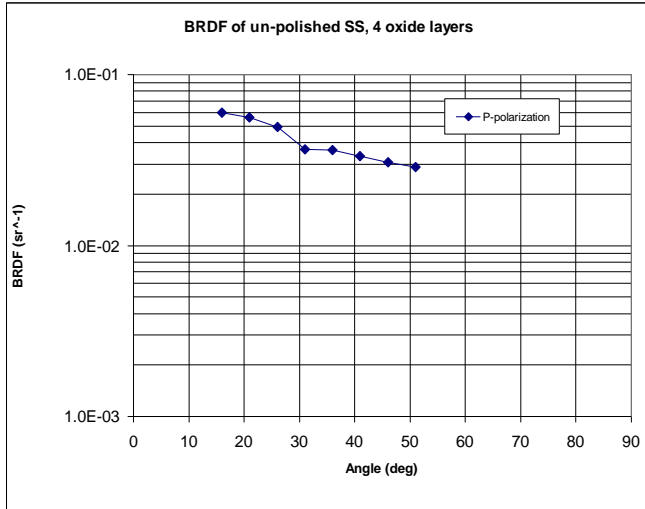


Figure 15 – BRDF of un-polish stainless steel with 4 oxide layers

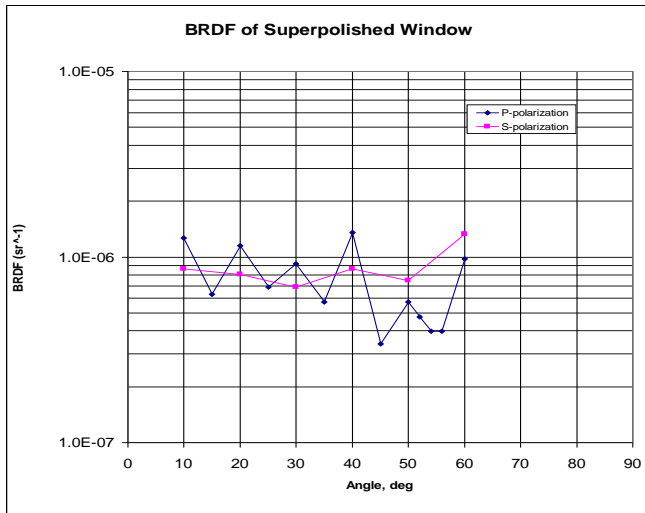


Figure 16 – BRDF of superpolished window



## APPENDIX B

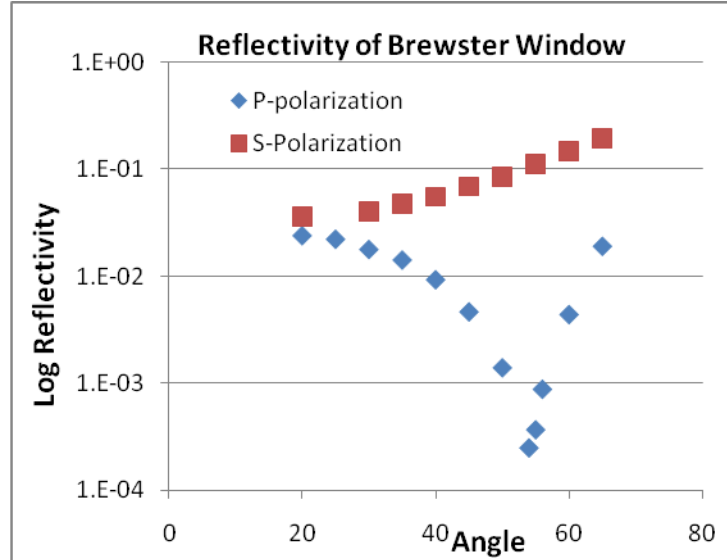
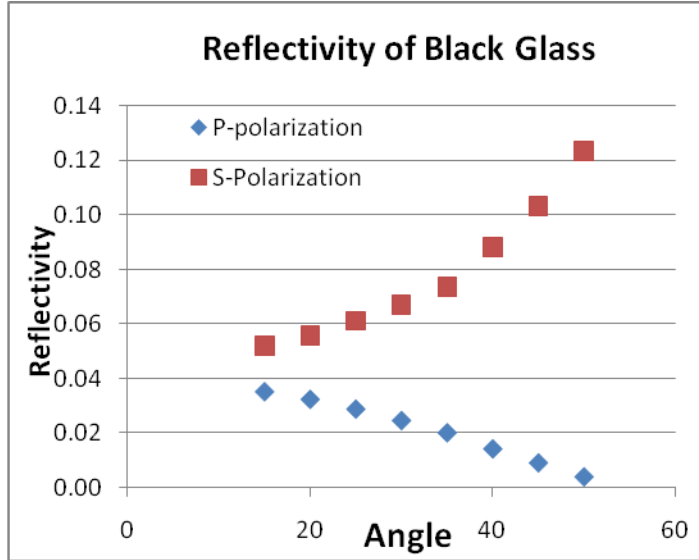
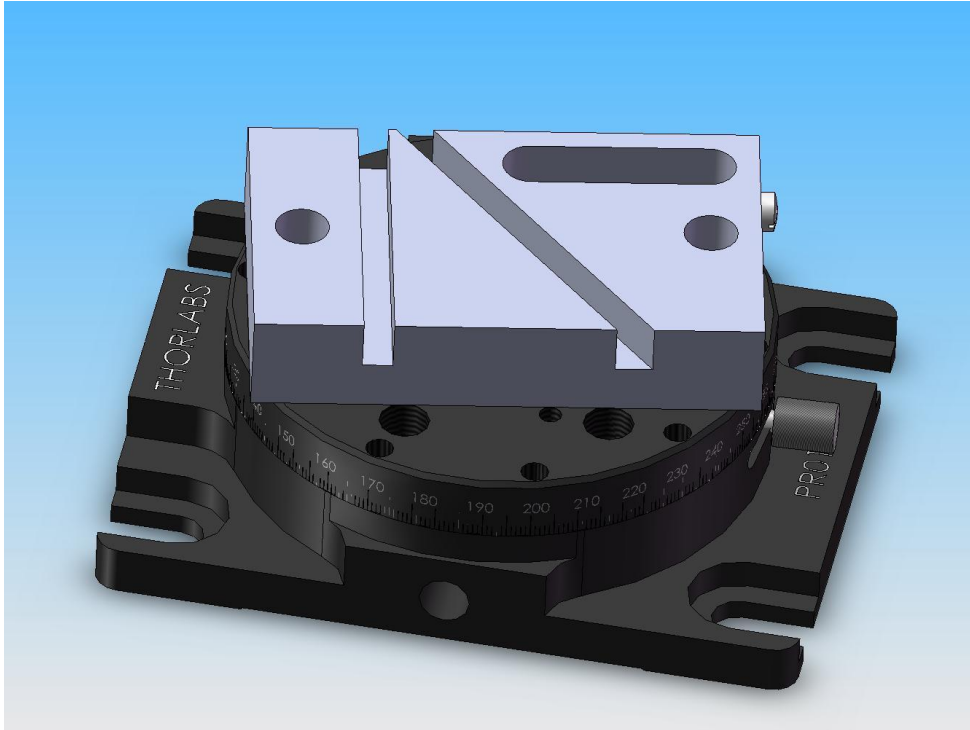


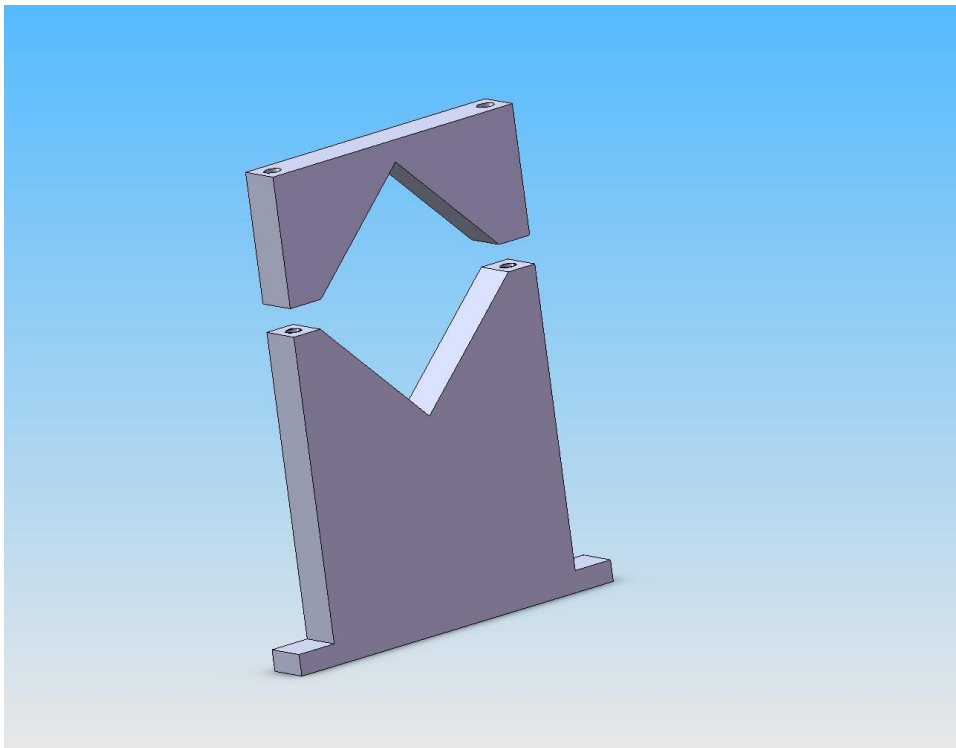
Figure B 2 - Brewster Window Reflectivity

Figure B 1 - Black Glass Reflectivity

## APPENDIX C



**Figure C 1 - Sample Mount and Rotational Stage**



**Figure C 2 - Telescopic Lens Mount**

## APPENDIX D

### MATLAB PROGRAM FOR GAUSSIAN BEAM PROPOGATION

```

%% Program to determine beam waist radius and location
%%
% Created from a program written by Mike Smith and converted to
Matlab by Dan Riley
%% Enter the parameters of the system
lamda = 1.064e-3;           %Laser wavelength, mm
w1 = .1;                   %Initial laser beam waist, mm
f1 = -170;                 %Focal length of the first
lens, mm
f2 = 150;                 %Focal length of the second
lens, mm
L1 = 200;                 %Distance from laser beam
waist to the first lens, mm
L2 = 97.363;             %Distance between the two
lenses, mm
L3 = 650.632;           %Distance from second to the
sample

%% Enter the upper and lower limits for the distance between the
two lenses
LF = 1;
UF = 130;
%%
% The matrices to describe the optical elements are multiplied
MT1 = [1 L1; 0 1];       %First translation matrix
ML2 = [1 0; -1/f1 1];    %First lens matrix
MT3 = [1 L2; 0 1];       %Second translation matrix
ML4 = [1 0; -1/f2 1];    %Second lens matrix

```

```

M14 = ML4*MT3*ML2*MT1;           %System matrix for the
first 4 elements
%%
% The Location of the beam waist is calculated
LBW3 = (-(((pi*w1^2)/lamda)^2)*M14(2,1)*M14(1,1) -
M14(1,2)*M14(2,2))/...
      (((pi*w1^2)/lamda)^2)*M14(2,1)^2+M14(2,2)^2);           %Beam
waist location calculation

%%
% The full system matrix is calculated
MT5 = [1 LBW3; 0 1];           %Third translation matrix
using beam waist location
M15 = MT5*ML4*MT3*ML2*MT1;           %Full system matrix using
beam waist location - All 5 elements
%%
% The beam waste radius is calculated
wBW2 = ((lamda/pi)*(-(M15(1,2)^2) -
(M15(1,1)^2)*((pi*w1^2)/lamda)^2))/...
      (((pi*w1^2)/lamda)*(M15(1,2)*M15(2,1) -
M15(1,1)*M15(2,2))))^(1/2);           %Calculation of laser radius at
the beam waist

%%
% The beam waste radius at the sample location is calculated
MT5 = [1 L3; 0 1];           %Third translation matrix
M15 = MT5*ML4*MT3*ML2*MT1;           %Full system matrix - All 5
elements

w2 = ((lamda/pi)*(-(M15(1,2)^2) -
(M15(1,1)^2)*((pi*w1^2)/lamda)^2))/...
      (((pi*w1^2)/lamda)*(M15(1,2)*M15(2,1) -
M15(1,1)*M15(2,2))))^(1/2);           %Calculation of laser radius at
L3

```

```

%% The data output of the calculations
disp(['If the distance between the lenses is: ',num2str(L2)])
disp(['The laser beam waist is located at: ',num2str(LBW3)])
%Displays the location of the beam waist
disp(['The laser beam waist radius is: ',num2str(wBW2)])
%Displays the laser beam waist radius
disp(['If the sample is located at: ',num2str(L3)]) %Displays the
location of the sample
disp(['The radius of the beam at the sample is: ',num2str(w2)])
%Displays the location of the sample
%%
% The data for the plots are generated in this "for" loop
for m=LF:UF
    xBW(m)=m;
    L2 = m;
    MT1 = [1 L1; 0 1]; %First translation matrix
    ML2 = [1 0; -1/f1 1]; %First lens matrix
    MT3 = [1 L2; 0 1]; %Second translation
matrix
    ML4 = [1 0; -1/f2 1]; %Second lens matrix

    M14 = ML4*MT3*ML2*MT1; %System matrix for the
first 4 elements

    LBW3 = (-(((pi*w1^2)/lamda)^2)*M14(2,1)*M14(1,1)-
M14(1,2)*M14(2,2))/...
        (((pi*w1^2)/lamda)^2)*M14(2,1)^2+M14(2,2)^2); %Beam
waist location calculation
    yLBW3(m) = LBW3;

    MT5 = [1 LBW3; 0 1]; %Third translation
matrix using beam waist location
    M15 = MT5*ML4*MT3*ML2*MT1; %Full system matrix
using beam waist location - All 5 elements

```

```

    wBW2 = ((lamda/pi)*(-(M15(1,2)^2)-
(M15(1,1)^2)*((pi*w1^2)/lamda)^2)/...
    (((pi*w1^2)/lamda)*(M15(1,2)*M15(2,1)-
M15(1,1)*M15(2,2))))^(1/2); %Calculation of laser radius at
the beam waist
    ywBW2(m) = wBW2;
end

%% The beam waist location plot
plot(xBW,yLBW3)
xlabel('Focus length');
ylabel('Beam waist location');
title('Beam waist location versus focus length');
%% The beam waist radius plot
plot(xBW,ywBW2)
xlabel('Focus length');
ylabel('Beam waist radius');
title('Beam waist radius versus focus length');

```

## APPENDIX E

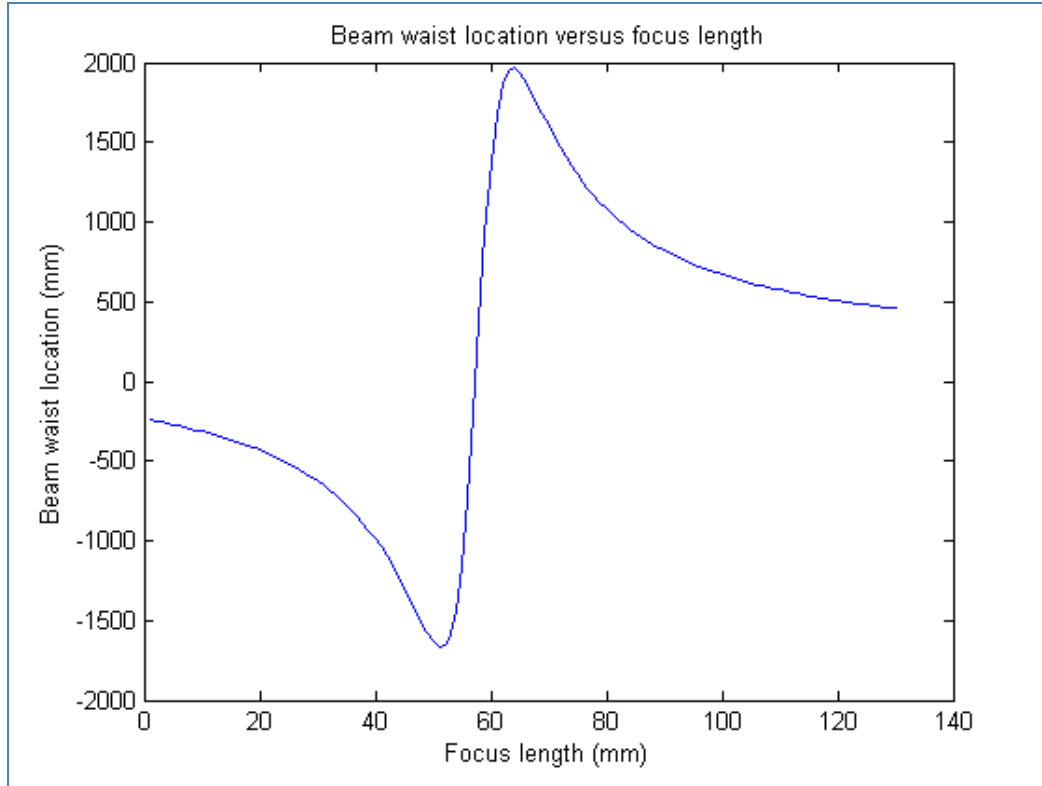


Figure E 1 - Plot of beam waist location versus focus length created using Matlab

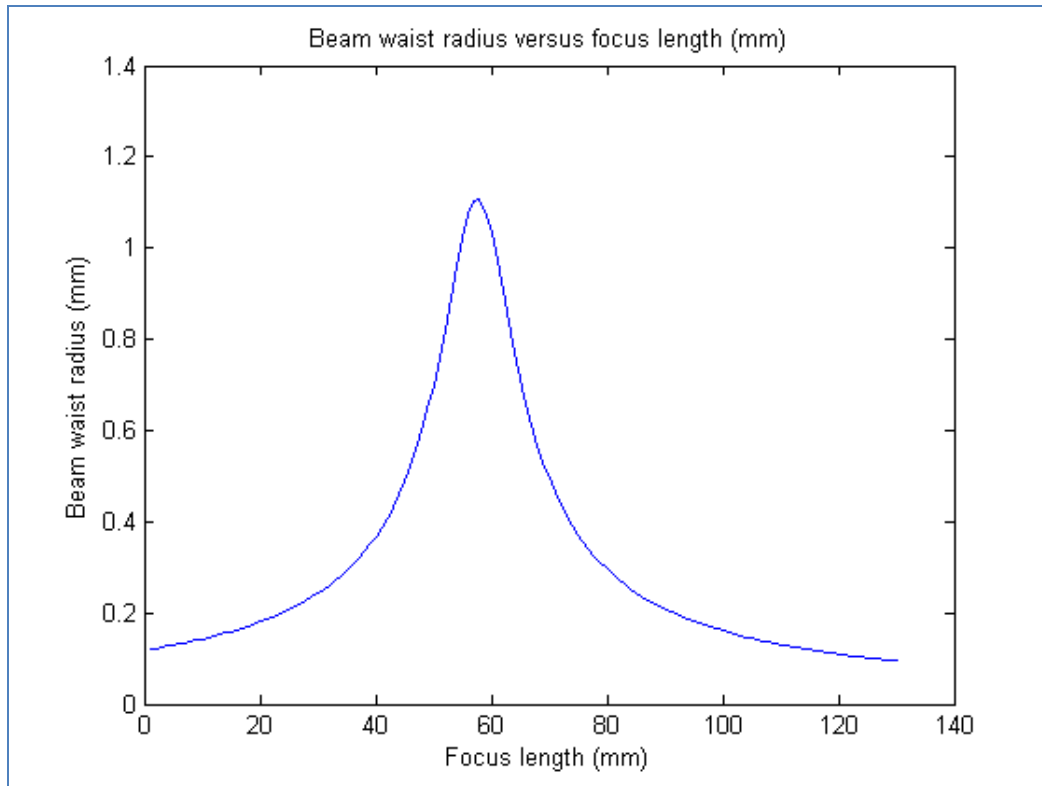
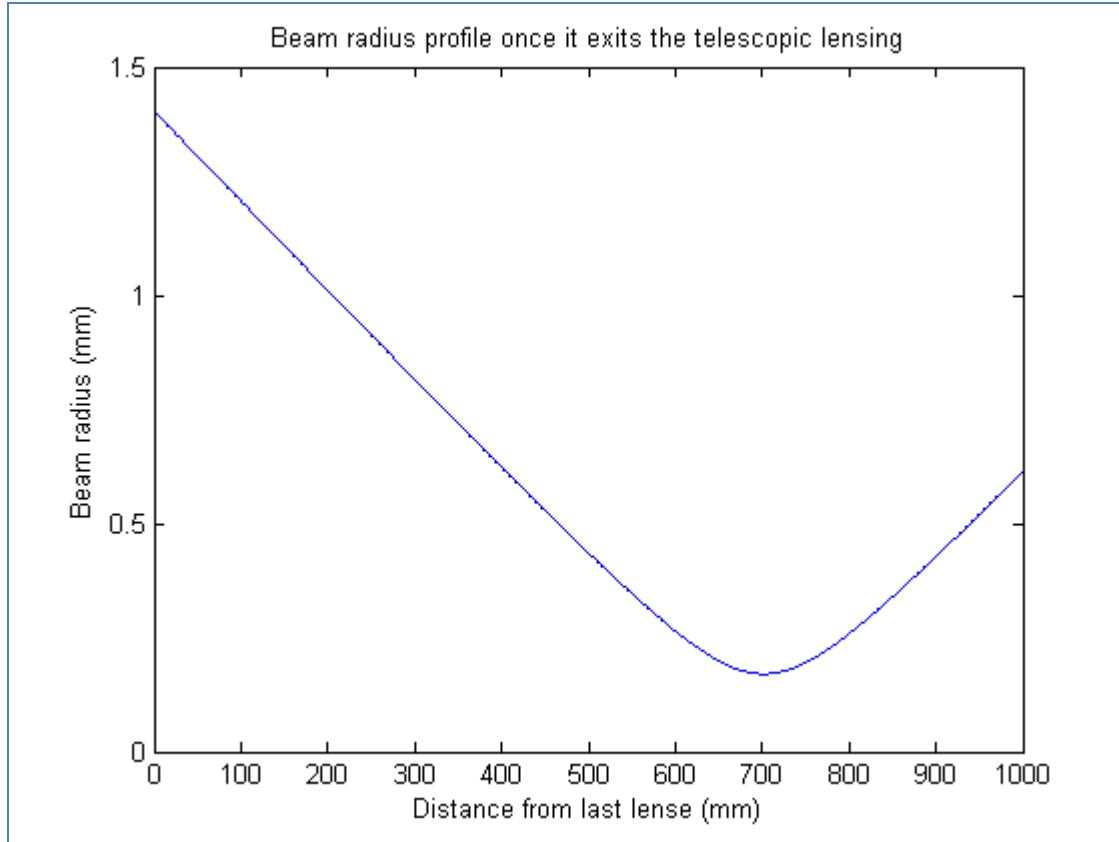


Figure E 2 - Plot of beam waist radius versus focus length created using Matlab





**Figure E 3 - The radius of the beam as it propogates through space once is exits the beam focus - Created with Matlab**